INTERNATIONAL JOURNAL OF SATELLITE COMMUNICATIONS AND NETWORKING
Int. J. Satell. Commun. Network. 2012; **30**:52–63
Published online in Wiley Online Library (wileyonlinelibrary.com). DOI: 10.1002/sat.1007

Advanced receiver design for satellite-based automatic identification system signal detection††

Paolo Burzigotti[1], Alberto Ginesi[1] and Giulio Colavolpe[2,*,†]

[1]*ESTEC European Space Agency, Noordwijk, The Netherlands*
[2]*Dipartimento di Ingegneria dell'Informazione, University of Parma, Parma, Italy*

SUMMARY

This paper describes an innovative receiver architecture for the satellite-based automatic identification system. The receiver performance has been fully validated in the presence of the typical satellite channel characteristics. In particular, it is shown that the devised receiver provides an excellent performance against the noise, as well as a large resilience against message collisions, Doppler shift, and delay spread. Copyright © 2012 John Wiley & Sons, Ltd.

Received 10 January 2012; Accepted 19 January 2012

KEY WORDS: satellite; LEO; AIS; maritime; demodulation; detection

1. INTRODUCTION

We present the design of an innovative receiver targeting reception of the automatic identification system (AIS) [1] signals from low earth orbit (LEO) satellites. A patent application has been filed at the European Patent Office for the receiver described in this paper.

The AIS communication system was initially developed to provide different type of information to vessels and shore stations, including position, identification, course, and speed. By means of a continuous traffic monitoring, the vessels can anticipate and thus avoid collisions in the sea. Furthermore, AIS also offers important ship-monitoring services to coastal guards or search and rescue organizations. However, the AIS system has a limitation in its range of coverage. Indeed, the protocol is designed such that the vessels operate in self-organized time-division multiple access (SOTDMA) regions, each coping with path delays no longer than about 200 nautical miles, with a typical radio frequency coverage limited to about 40 nautical miles. Within this range, all ships in visibility use the SOTDMA protocol, which ensures that collisions are prevented from bursts transmitted by different ships.

Today, there is an increasing interest in detecting and tracking ships at distances from coastlines that are larger than those that can be accomplished by normal terrestrial very high frequency (VHF) communications. Better handling of hazardous cargo, improved security, and countering illegal operations are examples of recent requirements of long range applications leading to the need to detect ships at very long distances from shores.

This work, together with [2], aims at demonstrating that a satellite-based AIS represents a promising solution to overcome the terrestrial VHF coverage limitation with the potential to provide AIS detection service coverage on any given area on the Earth. In particular, the design of the innovative receiver described in this paper must be considered as the building block of the satellite-based AIS detailed in [2].

*Correspondence to: Giulio Colavolpe, Dipartimento di Ingegneria dell'Informazione, University of Parma, Parma, Italy.
†Email: giulio@unipr.it
††The paper was presented in part at the 5th Advanced Satellite Mobile Systems Conference 11th International Workshop on Signal Processing for Space Communications (ASMS&SPSC 2010), Cagliari, Italy, September 2010.

The rest of the paper is organized as follows. In Section 2, it is shown that a satellite-based AIS has to face with severe technical challenges that were not considered in the original AIS standard [1], that is, (i) colliding messages from ships transmitting from different SOTDMA cells, (ii) high carrier Doppler, (iii) lower signal-to-noise ratio (SNR) values, and (iv) longer relative propagation channel delays among the population of ships in visibility at any given time. Section 3 will describe in detail the devised receiver, specifically designed to cope with all these issues and based on advanced signal processing techniques to increase its sensitivity. Section 4 will show its performance in terms of bit and packet error rate, greatly increased with respect to typically used maritime AIS receivers. Reference [2] complements this paper showing how this translates in a much higher value of average ship detection probability, which, in turn, implies that the number of deployed LEO satellites in the constellation is reduced given the same ship position reporting interval.

A number of projects funded by ESA and the European Commission as well as private initiatives are currently undergoing to analyze the concept of satellite reception of AIS signals. Some trials have also been carried out. Overall, it has been proved that the new system is feasible provided efficient receiver techniques are employed.

2. THE CONCEPT OF SATELLITE-BASED AIS

2.1. General

Automatic identification system is a universal shipborne system [1] aimed at improving the safety and efficiency of navigation and at helping to protect the marine environment. Its main purpose is to facilitate an efficient exchange of messages among ships and also among ships and shore stations. Such a system is designed to operate autonomously within a range of about 40 nautical miles. Any AIS-equipped ship periodically transmits short fixed-length TDMA messages including ship identification, location, course, speed, and other status information. The nearby AIS receivers on board of ships or shore stations detect this information, thus providing a comprehensive picture of the local environment, complementary to the radar information.

The same International Telecommunication Union recommendation [1] introduces also the concept of long-range applications of AIS, identifying goals, and achievements of such system, for example, obtaining position updates of ships on the open sea at the rate of twice per day and even once every hour. A satellite-based AIS system is a way of obtaining the aforementioned objectives. This would have a global coverage enhancing even further the requisite of safety and navigation monitoring. The localization of ships would then be achieved globally, allowing the creation of a real-time database of ship positions.

However, a satellite system calls for several technical issues and operational challenges. An LEO constellation of small size satellites is usually assumed for global coverage, with an altitude ranging from 600 to 1000 km. From such an altitude and with the beamwidth typical of on-board VHF antennas, the satellite field of view (FoV) spans over a few thousands of nautical miles. The first issue to be considered then is the reception of signals coming from many AIS transmitters that are not within AIS communication range. Each of them is autonomously organized in a SOTDMA scheme [1] to reduce the collision probability. However, when signals coming from different and not communicating AIS cells are received at the satellite, the probability of slot collisions increases.

2.2. Automatic identification system signal format

The ITU-R M.1371-2 standard [1] covers the description of the signal format transmitted by the ships. In summary, the already mentioned TDMA frame is organized as described in the Table 1.

Each frame is composed by 2250 slots where the ships can transmit their bursts. In this paper, the terminologies *burst*, *message*, or *packet* will be used to refer the information data that ships transmit in the TDMA slots. The TDMA structure is repeated on two frequency channels, and each ship transmitter hops continuously between them.

The signal format consists of a Gaussian minimum shift keying (GMSK) with BT product [3] between 0.4 and 0.5. In the following, we will denote by T the bit interval.

DOI: 10.1002/sat

Table I. Summary of the main AIS protocol parameters.

Multiple access method	Self-organized TDMA (SOTDMA)
TDMA frame length	60 s
Number slots in TDMA frame	2250
Burst structure	Training sequence: 24 bits Start flag: 8 bits Data: up to 168 bits FCS: 16 bits End flag: 8 bits Time buffer: 24 bits
Vessels reporting rate	Between 2 s and 6 min
Transmission power	12.5 W (class A transponders only)
Symbol rate	9.6 kbit/s
Operational frequency bands	VHF with two channels (161.971 and 162.025 MHz) of 25 kHz bandwidth each

AIS, automatic identification system; SOTDMA, self-organized time-division multiple access; TDMA, time-division multiple access; VHF, very high frequency.

2.3. Satellite automatic identification system main channel characteristics

A satellite-based AIS has to face with additional technical challenges that were not considered in the original AIS standard. These new issues arise because of the spaceborne nature of the new system.

- Messages collisions: The typical radius of a SOTDMA cell (where no message collisions take place) is around 40 nautical miles. The self-organized structure is however lost when messages transmitted by more than one SOTDMA cell are received. This is the case of a satellite-based receiver because of the fact that the satellite FoV covers a high number of SOTDMA cells. In these conditions, several messages can collide within the same time slot (see Figure 1). The messages collide with a different received power level and delay because of the different channel propagation over the satellite antenna coverage.
- Path delay: The length of the AIS messages was designed to face with differential propagation delays between messages from different ships up to 2 ms. Path delays among vessels and spacecraft vary, depending on the vessels' location and on the maximum satellite antenna footprint. A consequence of exceeding the buffer delay is that even bursts transmitted in different slots of the TDMA frames can collide (see Figure 1).
- Low SNR values: Because of higher path losses and depending on the particular satellite antenna gains, SNR values between 20 and 0 dB are expected.
- Multipath and atmospheric attenuation: Negligible at VHF frequencies. Because of the low frequency, channel measurement results show that the multipath takes place at very low elevation angles (because of reflections on the sea surface), and thus, it does not impact the performance of the system. In addition, because of the low symbol rate and short messages, the multipath expected at low elevation angles corresponds to very slow amplitude variation of the channel so that no specific receiver countermeasures are needed.

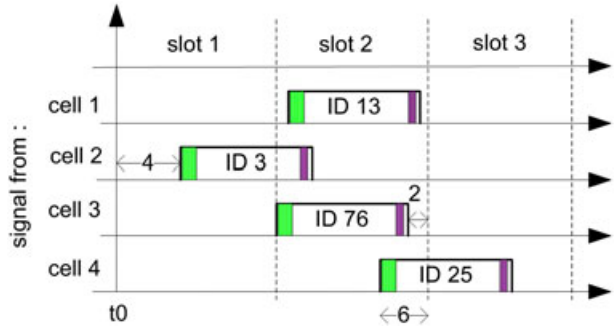

Figure 1. The message (burst) structure collision issue.

DOI: 10.1002/sat

- Faraday rotation: A linearly polarized wave entering the ionosphere may have a different polarization angle when it leaves. This polarization rotation is primarily dependent on frequency, elevation angle, geomagnetic flux density, and electron density in the ionosphere. When in the presence of a circularly polarized satellite receive antenna, a constant 3-dB loss is present when receiving the randomly rotated vertically polarized VHF wave as transmitted by the ship antenna.
- Doppler effect: The Doppler frequency shift is a function of the relative velocity between the transmitter and the receiver. In the case of the satellite-based AIS system, the ship velocity is small compared with the satellite, such that the Doppler shift can be calculated as $\Delta f = v_r/\lambda$, where $\lambda = c/f$ (= 1.86 m) is the wavelength of the original AIS signal and v_r is the component of the satellite velocity directed toward the ship. v_r will vary with elevation and azimuth angle from zero ($\Delta f = 0$) when the ship free line-of-sight to the satellite is orthogonal to the satellite velocity vector and to a maximum value with the ship placed just within the satellite local horizon and the free line-of-sight parallel to the satellite velocity vector. For typical LEO altitudes and FoV used in AIS applications, the maximum Doppler shift is around 4 kHz. Because of the symmetry of the coverage area, the Doppler shift then varies between −4 and +4 kHz with maximum relative Doppler between two messages of 8 kHz.

3. AUTOMATIC IDENTIFICATION SYSTEM SATELLITE RECEIVER ARCHITECTURE

3.1. Background

Typical low-cost implementations of commercial AIS receiver equipments are based on the so called two-bits differential demodulator. The advantage of this scheme is its extreme simplicity, its insensitivity to carrier phase errors, and its capability to demodulate signals with different *BT* values. Its application to spaceborne AIS systems has also been proposed in [4]. However, its performance in terms of bit error rate (BER) as a function of E_S/N_0 and its sensitivity to cochannel interference are not satisfactory to cope with the low SNR values and the message collision issue as described in Section 2.

3.2. Advanced automatic identification system satellite receiver

Figure 2 shows a detailed block diagram of the devised advanced AIS receiver for satellite reception. The main features of this receiver consist in the following:

- enhanced sensitivity with respect to white noise (4–5 dB better than the two-bit differential detector described in the previous section), which also translates into an equivalent improved sensitivity

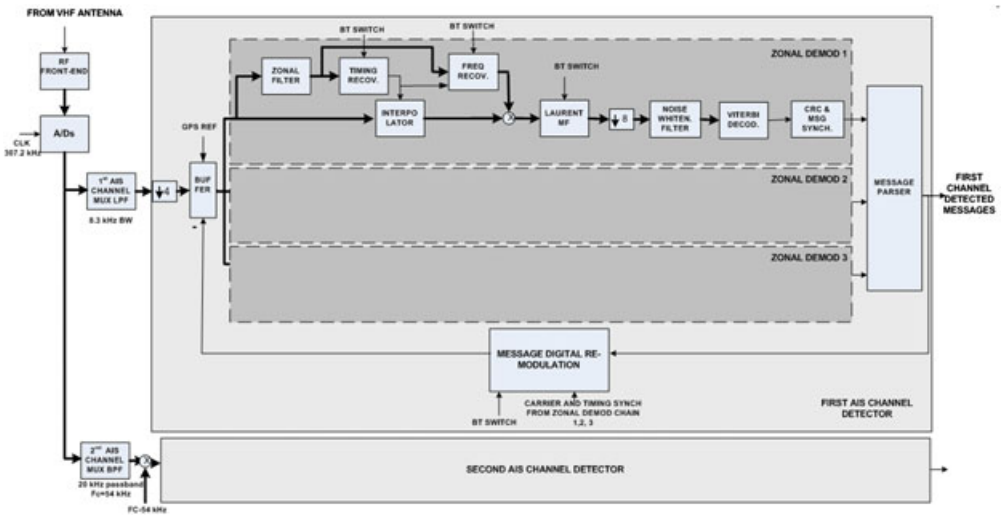

Figure 2. Architectural block diagram of the advanced automatic identification system satellite receiver.

DOI: 10.1002/sat

against interfering messages. This is achieved by using a noncoherent detector scheme [5],[6] whose performance approaches that of the optimal maximum-likelihood (ML) coherent scheme. Thanks to the noncoherent detection, phase recovery synchronization is not required;
- exploitation of the carrier frequency diversity generated by the Doppler spread within the satellite FoV. This is achieved by processing three contiguous different sub-bands within the total received signal bandwidth. This latter amounts to the ideal signal bandwidth (typically around the symbol rate) plus two times the max Doppler shift, that is, 4 kHz, for a total of about 18 kHz, and using an efficient carrier frequency recovery scheme;
- receiver insensitivity to the *BT* value of the GMSK signal transmitter;
- digital signal remodulation and interference cancelation to enhance the message collision resolution performance of the receiver. A message successfully decoded is remodulated and subtracted from the composite signal received in the TDMA slot under analysis. The resulting composite signal is then reprocessed by the receiver to 'extract' further messages. The iterative process is repeated until no more messages can be successfully decoded.

Following the diagram of Figure 2, the signal received from the VHF antenna is first processed by an analog radio frequency front end whose detailed description is out of the scope of this paper, but it basically consists of a low-noise power amplification followed by a two-stage frequency down-conversion and filtering to reach the baseband configurations as depicted in Figure 3.

A couple of A/D converters then sample the in-phase (I) and quadrature (Q) components of the signal at 32 times the bit rate of one channel (9.6 kbps), that is, 307.2 kHz. This choice allows to avoid signal aliasing at digital level and to relax the filtering requirements of the following AIS channel multiplexer (MUX) filters. Two AIS channel MUX filters are then used to separate the two channels

The digital clock rate can thus be reduced by a factor of 4 to obtain only eight samples per information symbol. This sampling rate is considered adequate for the next processing including the timing recovery. At the output of the decimation stage, a buffer is present to store a number of signal samples. From the buffer, a copy of all signal samples is read sequentially and input to the following zonal demodulators after the already decoded messages fully or partially fitting the considered TDMA slot are subtracted from them by the receiver feedback block called 'message digital remodulation'. The process loops continuously use the same signal samples until no more messages can be decoded.

The rationale of the 'zonal demodulators' is justified by the exploitation of the frequency diversity given by the Doppler spread. This is illustrated in Figure 4 where the overall AIS channel band is

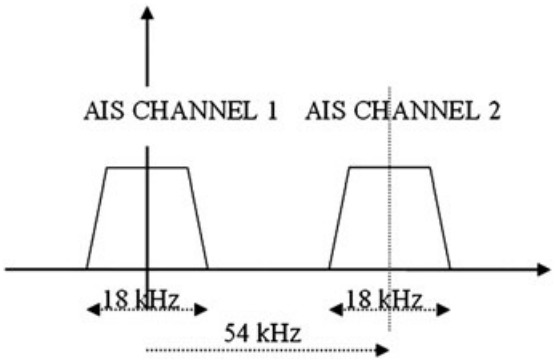

Figure 3. Baseband automatic identification system channels at the output of the radio frequency front end.

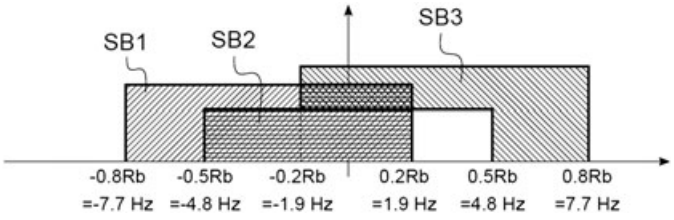

Figure 4. Automatic identification system channel sub-band partition.

DOI: 10.1002/sat

divided into three overlapping sub-bands, each of bandwidth equivalent to the signal bit rate R_b, and staggered by $0.3R_b$.

In particular, each zonal demodulator is specifically designed to process only one slice of the AIS channel and to achieve the target performance within that slice. However, so as not to distort the received signal to be decoded, the zonal filter is only applied to the signal to be used for timing and frequency recovery as described in Figures 2 and 5.

The outputs of the three zonal demodulators are connected to the message parser block, which is in charge of discarding duplicated messages and feed the digital remodulation block for message interference cancelation. Indeed, given the overlap between the AIS channel sub-bands, it might occur that the same message is successfully decoded by more than one zonal demodulator.

3.3. Zonal demodulator

Each zonal demodulator takes as an input the samples from the buffer after cancelation and then carries out the basic synchronization and detection functions. In particular, it consists of timing and carrier frequency synchronization block (TCS), the noncoherent sequence detector block (NCSD), and the frame synchronization and CRC verification block (FSCV). Most of the algorithms in the zonal demodulator depend on the actual value of the BT product of the incoming message. It will be shown later that the performance of the devised demodulator is practically insensitive to the actual BT value of the received signal provided its actual value is in the range $[0.3, 0.6]$, when it is assumed that the demodulator has been designed for $BT = 0.4$ (nominal value).

3.3.1. Timing and carrier frequency synchronization block. The block diagram of the TCS component of the zonal demodulator is shown in Figure 5. Timing and carrier frequency compensations are performed before the NCSD block. Correct signal timing epoch and carrier frequency are derived by means of timing and frequency recovery algorithms detailed in the succeeding paragraphs. These algorithms are fed by the TCS input data signal further preprocessed by a narrow low pass (LP) filter. The purpose of this TCS-LP filter is to limit as much as possible the interference from AIS signals with a Doppler shift large enough to fall within the frequency band of successful demodulation of an adjacent AIS signal sub-band associated to another zonal demodulator. In that respect, it acts as a zonal demodulator MUX filter, although outside the signal data path. This choice has been derived from the experimental observation that the synchronization algorithms are less sensitive to signal distortions because of the narrow TCS-LP filter than the performance of the NCSD block.

The timing and carrier synchronization functions are carried out over a window of only 128 symbols (bits) belonging to the TDMA slot in the middle of the buffer. The reason for this is that the current message alignment is not known at this point, so the synchronization blocks have to be activated on the portion of the slot where messages transmitted in those slots would have energy for sure. It turns out that, given the max differential delay between messages in the coverage, only 128 symbols of the slot can be used.

Timing recovery is needed at this stage because the following frequency recovery takes advantage of the optimum sampling time. This algorithm has a feedforward structure and is well suited for reception

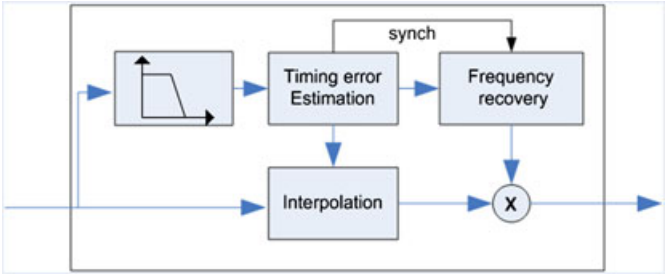

Figure 5. Timing and carrier frequency synchronization block.

DOI: 10.1002/sat

of burst-type signals. The solution described in [7] has been tailored to the specific application considered for this paper. Particularly, GMSK modulation with a BT factor equal to 0.4 has been considered.

As it will be shown later, the maximum tolerable residual carrier offset at the NCSD input has been experimentally estimated in $0.02R_b$. Thus, the task of the carrier frequency recovery algorithm is to lower the carrier frequency offset from the maximum of $0.15R_b$ (recall than the three zonal demodulators are spaced in frequency of $0.3R_b$) to at most $0.02R_b$.

The frequency recovery scheme uses the signal resampled in time to the optimum instant (clock-aided scheme) and derives the carrier frequency estimation on the basis of the feedforward structure detailed in [7].

3.3.2. Noncoherent sequence detector block. The scheme described in [5],[6] has been used as data detector, thanks to the following key features: (i) excellent BER performance, that is, very close to the ideal coherent ML detector performance, (ii) insensitivity w.r.t. carrier phase: because of the short length of the AIS messages, the accuracy of phase recovery schemes may significantly degrade the detector BER performance, and (iii) high resilience w.r.t. carrier frequency offsets, thanks to the noncoherent approach.

The input signal, that is, the output of the TCS block at eight samples per bit, is first filtered by a filter matched to the first component of the Laurent expansion of the GMSK signal. For a GMSK signal with $BT = 0.4$, most of the energy is within the first pulse; thus, the signal can be fairly well approximated by the first Laurent component.

The output of the Laurent matched filter is down sampled to one sample per symbol (bit) and fed to a whitening filter whose purpose is to whiten the noise that has been shaped by the Laurent matched filter [5],[6]. This filter is a simple finite impulse response (FIR) filter with five taps.

A ($S = 2$) two-state Viterbi decoder then follows the whitening filter. The relevant branch metrics are described in [5],[6]. A value of $N = 4$ of the implicit memory parameter 5,6 has been selected.

3.3.3. Frame synchronizer and CRC verification block. The block diagram of the FSCV block is shown in Figure 6. Starting from the consideration that frame synchronization based only on the Start-of-Flag field of the AIS message would be not reliable enough in interference-limited systems as all messages use the same Start-of-Flag field, the alignment to the start of the message is achieved by computing the cyclic redundancy check (CRC) for the 128 possible start positions of the message. When the right position is found, the CRC is verified and the successfully decoded message is passed on to the message parser block. To lower the probability of false alarm down to an acceptable value, a Start-of-Flag verification is also performed.

3.4. Interference cancelation. Interference cancellation mechanism is triggered for every successfully decoded message at the output of the AIS channel detector. A baseband message is digitally reconstructed by remodulating the decoded bits. Then, the estimated timing alignment, phase, and frequency are applied before the cancelation from the received signal.

Because noncoherent decoding is carried out in the zonal demodulator and a relatively large residual carrier frequency offset may be estimated by the frequency recovery scheme (the noncoherent decoder can operate with frequency errors up to $0.02R_b$), a refined frequency estimate [8] as well as a carrier

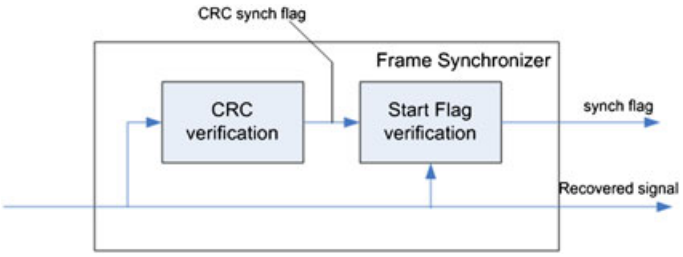

Figure 6. Block diagram of the frame synchronization and CRC verification block.

DOI: 10.1002/sat

phase estimate [9] is required for a sufficiently precise interference cancelation. This is accomplished through data-aided algorithms by using the whole detected burst.

This procedure is iterated until messages out of the SOTDMA slot under analysis are being successfully decoded.

3.4.1. Digital remodulator. Figure 7 shows the block diagram of the modulator needed to digitally remodulate the successfully decoded message. The main features of this receiver consist in the following:

1. the input signals are
   (a) same input as for the NCSD but with timing and frequency correction already performed and
   (b) successfully decoded messages (bit data);
2. the devised blocks perform a refinement of timing, frequency, phase, and amplitude estimation on the basis of the knowledge of the received signal (data-aided algorithms);
   (a) initial frequency error up to $0.02R_b$, time alignment error up to $1/(8R_b)$ are considered;
   (b) the estimation algorithms are based on the ML approach;
3. the decoded message output of the zonal demodulators is then digitally remodulated and fed back to be canceled from the receiver input.

4. PERFORMANCE

The performance of the NCSD block over the additive white Gaussian noise (AWGN) channel, in terms of BER curve, is reported in Figure 8. In all figures but Figsures 12 and 13, ideal synchronization

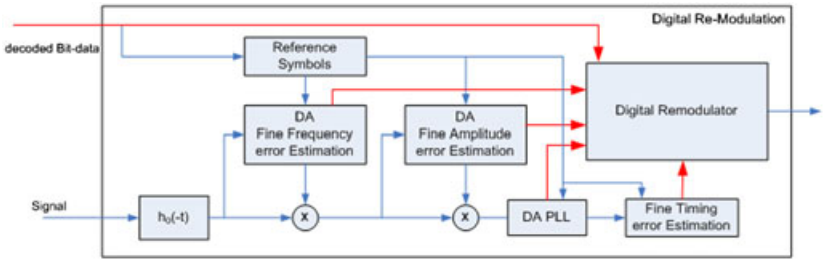

Figure 7. Architectural block diagram of the digital remodulator.

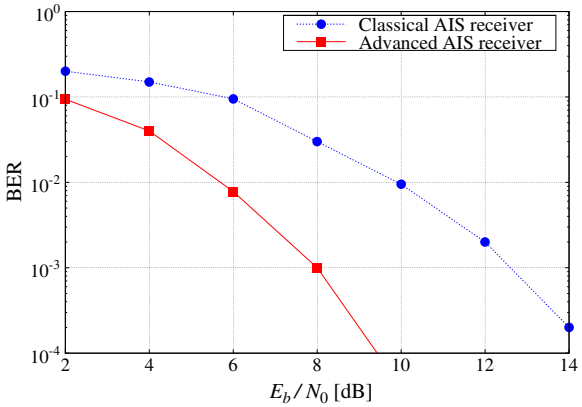

Figure 8. Bit error rate of the advanced receiver on the additive white Gaussian noise channel with no interference and ideal synchronization and comparison with that of a two-bit differential detector.

DOI: 10.1002/sat

is assumed. However, we found no loss associated to the adoption of the described timing and frequency synchronization algorithms even in the presence of strong interference. In that case, in fact, inteference mainly affects the performance of the detection algorithm so the impact on the synchronization algorithms is negligible.

Also of interest is the interference rejection performance of the advanced receiver with ideal synchronization. To this respect, Figures 9 and 10 show the BER performance in the presence of a variable number (from 0 to 5) of cofrequency interfering signals with the same power. When the interfering signals are present, the *C/I* (signal-to-overall-interference power ratio) is always set to 5 dB (Figure 9) or 10 dB (Figure 10). From these figures, it turns out that decoding of messages colliding with a relatively low signal-to-interference power is still possible provided the SNR is high enough. For example, an E_S/N_0 of at least 18 dB guarantees a BER of less than 10^{-2} when one interfering signal only is present, and thus a packet error rate (PER) of less than 1, thus enabling ship message detection after a number of transmissions. For example, if the PER is 0.9, after 20 received messages from the same ship, the probability that a ship message is not detected is 0.9^{20}, that is, about 0.12. From the same figure, it is also evident that, for a given *C/I*, the performance worsens with the number of interfering signals. This is expected because when the number of interfering signals grows, the interference distribution tends to widen and becomes Gaussian, thus impacting more the performance.

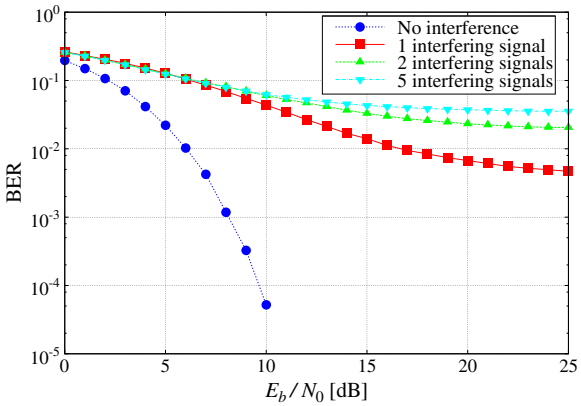

Figure 9. Bit error rate of the advanced receiver with ideal synchronization and with a variable number of interfering signals (total $\boldsymbol{C/I = 5}$ dB).

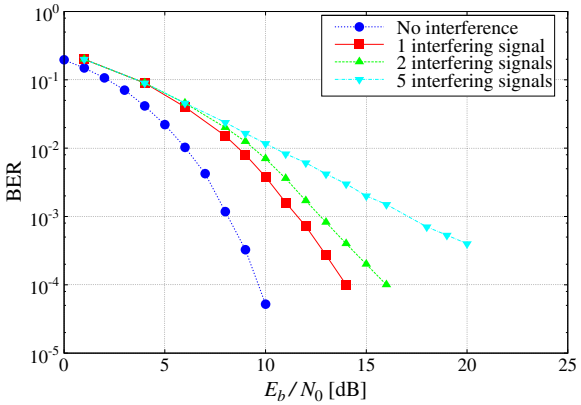

Figure 10. Bit error rate of the advanced receiver with ideal synchronization and with a variable number of interfering signals (total $\boldsymbol{C/I = 10}$ dB).

DOI: 10.1002/sat

Figure 11 shows the sensitivity to the carrier frequency offset of the interfering message. As expected, when the interference is offset in frequency with respect to the main message, the BER performance improves notably. This is because of the interference rejection capability of the NCSD block.

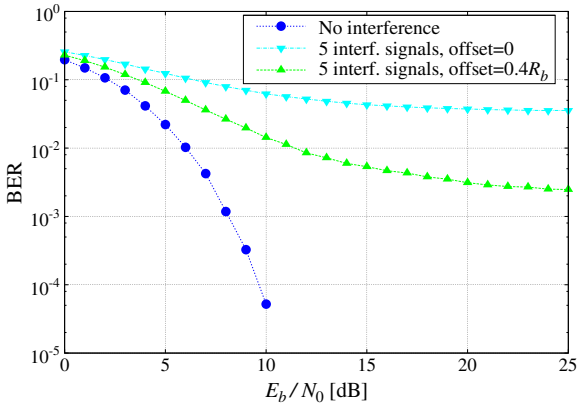

Figure 11. Bit error rate of the advanced receiver with ideal synchronization when in the presence of five interfering signals with $\boldsymbol{C/I = 5}$ dB and different carrier frequency offsets (0 and $\boldsymbol{0.4R_b}$).

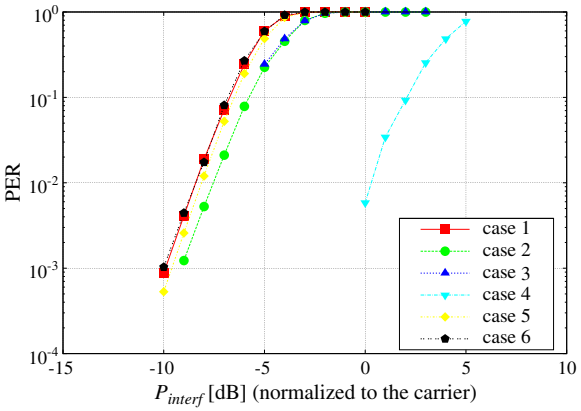

Figure 12. Packet error rate of the advanced receiver with one interfering signal and different ***C/I***, frequency shifts, and power levels of the two colliding messages.

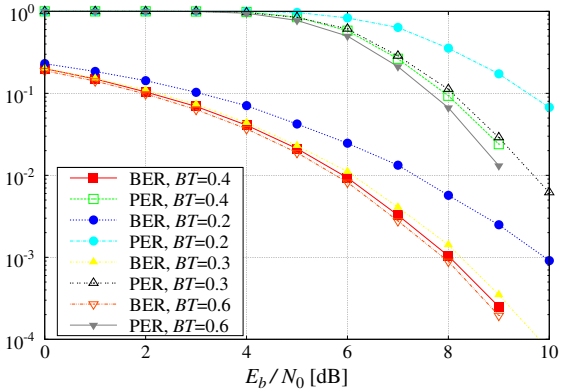

Figure 13. Sensitivity to different transmitted BT values, when the expected value is $\boldsymbol{BT = 0.4}$.

DOI: 10.1002/sat

The performance of the proposed receiver has been tested in selected cases to cover several combinations of target-signal and interfering-signal frequency offsets. In particular, the receiver performance has been verified setting the E_s/N_0 according to the worst case level calculated via link budget, $E_s/N_0 = 15$ dB and against different interfering signal power levels. In particular, the following cases have been defined:

Case 1: $\{F_{signal}, F_{interf}\} = \{0, 0\}$ kHz	Case 2: $\{F_{signal}, F_{interf}\} = \{0, -4\}$ kHz
Case 3: $\{F_{signal}, F_{interf}\} = \{-1.5, 4\}$ kHz	Case 4: $\{F_{signal}, F_{interf}\} = \{-3, 4\}$ kHz
Case 5: $\{F_{signal}, F_{interf}\} = \{-0.75, 2\}$ kHz	Case 6: $\{F_{signal}, F_{interf}\} = \{-1.5, -1.5\}$ kHz

As it can be easily derived from Figure 12, the pairs {case 1, case 6} and {case 2, case 3} present identical results to confirm that the performance is interference-limited, and it is not affected by the synchronization algorithms. Indeed, within one pair, the associated interference power, and therefore *C/I*, is (almost) constant, whereas the synchronization performance is affected by the different distortion introduced by the filter in TCS (because of the relative position). A performance improvement can be achieved through frequency discrimination, thanks to the Doppler effect, for example, case 1 versus case 3 or case 4. However, this improvement is ruled by the maximum interference rejection of the NCSD block as a function of the relative carrier offset (useful signal vs. interfering signal).

As anticipated, because of the limited accuracy of the on-board ship transmitters, the GMSK waveform may present a *BT* value different from the nominal expected $BT = 0.4$. The proposed solution shows a performance practically insensitive to the actual transmitted *BT*, provided that it is within the reference range $[0.3, 0.6]$ as shown in Figure 13, where the performance analysis in terms of sensitivity to different transmitted *BT* values, when the expected value is $BT = 0.4$, is reported. It clearly appears that a degradation is experienced only when the actual transmitted value is out of the possible range, nominally $BT = 0.2$. On the contrary, no losses have been observed for *BT* within $[0.3, 0.6]$.

5. CONCLUSIONS

This paper describes an innovative receiver design for satellite AIS systems. A patent application has been filed at the European Patent Office. The paper shows that the devised receiver has an excellent performance in terms of enhanced sensitivity to noise floor, excellent resilience to interference, insensitivity to the value of *BT* and capability to exploit carrier frequency shift as source of diversity. All this makes the described design innovative and well suited for AIS satellite systems. In [2], it is shown how this advanced design can be exploited as building block of a complete satellite-based vessel AIS, with a much higher value of average ship detection probability with respect to conventional receivers. In turn, this implies a strongly reduced number of deployed LEO satellites in the constellation, given the same ship position reporting interval.

REFERENCES

1. Technical characteristics for an automatic identification system using time division multiple access in the VHF maritime mobile band. Recommendation ITU-R M.1371-2. April 2010
2. Cervera MA, Ginesi A, Eckstein K. Satellite-based vessel Automatic Identification System: a feasibility and performance analysis. *International Journal of Satellite Communications and Network*. 2011; **29**(2):117–142.
3. Murota K, Hirade K. GMSK modulation for digital mobile radio telephony. *IEEE Transactions on Communications* 1981; **29**:1044–1050.
4. Hicks JE, Clark JS, Stocker J, Mitchell GS, Wyckoff P. AIS/GMSK receiver on FPGA platform for satellite application. *Proceedings of SPIE* 2005; **5819**. doi:10.1117/12.606 714.
5. Colavolpe G, Raheli R. Noncoherent sequence detection. *IEEE Transactions on Communications* 1999; **47**:1376–1385.
6. Colavolpe G, Raheli R. Noncoherent sequence detection of continuous phase modulations. *IEEE Transactions on Communications* 1999; **47**:1303–1307.
7. Morelli M, Mengali U. Joint frequency and timing recovery for MSK-type modulation. *IEEE Transactions on Communications* 1999; **47**:938–946.
8. Luise M, Reggiannini R. Carrier frequency recovery in all-digital modems for burst-mode transmissions. *IEEE Transactions on Communications* 1995; **43**:1169–1178.
9. Mengali U, D'Andrea AN. *Synchronization Techniques for Digital Receivers (Applications of Communications Theory)*. Plenum Press, New York, 1997.

DOI: 10.1002/sat

AUTHOR'S BIOGRAPHIES

Paolo Burzigotti was born in Italy in 1976. He received the Master's degree in Electronic Engineering, major subject in Telecommunications, from the University of Perugia, IT, in 2001. From 2001 to 2005, he was employed as communication system engineer in Space Engineering S.p.A, (Rome, IT) in the Digital Technology Department, where he worked on the development of digital receiver and transmission system. His main research interest include design of algorithms for telecommunication digital systems via satellite and feasibility analysis in hardware projects related to high-rate and high-order modulation modems. In 2006, He joined ESA's Research and Technology Centre (ESTEC), Noordwijk, The Netherlands, as a communication system engineer in the RF payload and systems, division. His current interests are mainly related to advanced mobile satellite communication systems design and optimization.

A. Ginesi was born in Parma, Italy, in November 1967. He received the Dr. Ing. cum laude) and Ph.D degrees in electronic engineering from University of Pisa, Italy, in 1993 and 1998, respectively. In 1996-1997 he spent one year at Carleton University, Ottawa, Canada, doing research on digital transmissions for wireless applications. In 1997, he joined Nortel Networks and in 2000 Catena Networks, both in Ottawa, Canada, where he worked on Digital Subscriber Loop (DSL) technologies and contributed to the definition f the second-generation ADSL standard. Since 2002 he joined ESA Research ad Technology Centre (ESTEC), Noordwijk, The Netherlands, where he is currently covering the position of the Head of the Communication-TT&C Systems & Techniques Section. His main current research interests lie in the area of advanced digital satellite communication systems and techniques from theory to HW implementation.

Giulio Colavolpe was born in Cosenza, Italy, in 1969. He received the Dr. Ing. degree in Telecommunications Engineering (cum laude) from the University of Pisa, in 1994 and the Ph.D. degree in Information Technologies from the University of Parma, Italy, in 1998. Since 1997, he has been at the University of Parma, Italy, where he is now an Associate Professor of Telecommunications at the Dipartimento di Ingegneria dell'Informazione (DII). In 2000, he was Visiting Scientist at the Institut Eur\'ecom, Valbonne, France. His research interests include the design of digital communication systems, adaptive signal processing (with particular emphasis on iterative detection techniques for channels with memory), channel coding and information theory. His research activity has led to more than 150 papers in refereed journals and in leading international conferences, and 15 industrial patents. He received the best paper award at the 13th International Conference on Software, Telecommunications and Computer Networks (SoftCOM'05), Split, Croatia, September 2005, the best paper award for Optical Networks and Systems at the IEEE International Conference on Communcations (ICC 2008), Beijing, China, May 2008, and the best paper award at the 5th Advanced Satellite Mobile Systems Conference and 11th International Workshop on Signal Processing for Space Communications (ASMS&SPSC 2010), Cagliari, Italy. He is currently serving as an Editor for IEEE Transactions on Wireless Communications and IEEE Wireless Communications Letters and as an Executive Editor for Transactions on Emerging Telecommunications Technologies (ETT).

DOI: 10.1002/sat